

ESTIMATION OF BIOLOGICAL LAYER THICKNESS AND REFRACTIVE INDEX OF SPR SENSORS USING NEURAL NETWORKS

TIAGO A. T. SOUSA^{†*}, ANTONIO M. N. LIMA[†]

**Instituto Federal de Alagoas, Palmeira dos Índios - AL, Brazil*

†Graduate Program in Electrical Engineering - PPGEE

Department of Electrical Engineering - DEE

Universidade Federal de Campina Grande - UFCG

Rua Aprígio Veloso, 882, 58429-900 Bairro Universitário

Campina Grande, Paraíba, Brazil

Emails: tiago.sousa@ee.ufcg.edu.br, amnlima@dee.ufcg.edu.br

Abstract— A simultaneous estimation of thickness and refractive index of the biological layer of the layer structure is still a problem for the use of optical biosensor based on SPR phenomenon. A study of the morphological parameters of the characteristic curve of the phenomenon and identification of its variation during the formation of the biological layer was applied in a neural network as prior knowledge. With this multiple prior knowledge a neural network could be trained estimate the quantities the parameter of interest ensuring a uniqueness to the solution.

Keywords— Surface plasmon resonance, neural network, system identification, bio-inspired systems.

Resumo— A estimação simultânea da espessura e do índice de refração da camada biológica do complexo de camadas ainda é um problema à utilização de bio-sensores ópticos baseados no fenômeno SPR. Através de um estudo dos parâmetros morfológicos da curva característica do fenômeno e da identificação de sua variação durante a formação da camada biológica possibilitou o uso de uma rede neural na qual pudessem ser inseridas as informações adquiridas no estudo morfológico da curva. Os conhecimentos prévios permitiram o treinamento da rede para estimar as grandezas de interesse garantindo a unicidade da solução.

Palavras-chave— Ressonância de plasma de superfície, rede neural, identificação de sistemas, sistemas bio-inspirados.

1 Introduction

Some optical bio-sensing techniques are described in literature. Among them those based on the Surface Plasmon Resonance (SPR) phenomenon and fluorescence phenomena are more relevant (Homola, 2003). The latter one is more selective and sensitive, however, the SPR technique enables the highest label free sensitivity and selectivity. The technique consists in creating a multi-layer arrangement favorable to the occurrence of the SPR phenomenon. The multi-layer complex is formed by: a high refractive index optical substrate; a metal layer, usually gold; a biological layer that immobilizes substance to be analyzed; and an external medium layer, air or water. A light focused on the layer complex excites the phenomenon and is reflected with some variations according to the formed layer. Detect these variations is useful to characterize the formed layer complex.

The SPR biosensor has great versatility of applications since its biological layer can be prepared to immobilize a most diverse group of substances. Determined the reaction to be analyzed the main difficulty in using the SPR biosensor consists in determining a combination of substances sensitive to the reaction that adhere to metallic layer. To detect a viruses, for example, a substances that bind to the antibody and gold is necessary.

The SPR technique has been used for over

two decades, but its limitations are not fully characterized. One of the most important characteristics of the SPR technique which is not yet fully understood is its capability for determining simultaneously the thickness and refractive index of the biological layer. This study addresses specifically this issue.

To simultaneously characterize both the thickness and refractive index of biological layer reduces the estimation error since each property influences the other. The correct characterization of biological layer also has some benefits in terms of increasing the sensitivity of the SPR biosensor; a study of the kinetics of layer formation; a determination of when the layer is ready to start sensing, reducing waste of solutions; and an identifying of imperfections in the layer formed.

Some solutions have been proposed to solve the problem, however each solution has its specific limitation. One of these solutions is based on data fitting techniques according to a bio-sensor model result of Fresnel equations. It is limited to a biological layer up to 2 nm (Phelps and Taylor, 1996). Other solution is to vary a fixed parameter of the system and get a result for each value of this parameter. By crossing data results in a single solution can be determined. The parameters can be: the solvent used in the external layer; the metal layer thickness (de Bruijn et al., 1991); exciting light, its wavelength or incidence an-

gle (Peterlinza and Georgiadis, 1996; Zhang and Wang, 2009; Johnston et al., 1995). These solutions are limited in application since they require changes to the system and/or data acquisition.

Characterize both the biological layer's refractive index and thickness is the main objective of the present paper. The characterization must be performed simultaneously and using only the measured SPR biosensor response curve, the SPR curve. This way a general solution to the problem is determined. Its application includes real-time monitoring of the layer, determination when the layer is fully formed, and identification of a wasted layer. The solution proposed in this paper is based only on the SPR curve and its morphological features so that it does not required any specific system modification.

2 Methodology

A simultaneous estimation of the refractive index and thickness of the biological layer using data only from the SPR curve has its main problem in the non-uniqueness of the answer. The data is composed by aa insufficient number of parameters. So that solutions obtaining different data samples by crossing excitation are so popular, as example two light sources at different frequencies. The non-uniqueness generates disagreements in the literature on whether an estimate based only on the SPR curve is possible or not.

The problem was studied focusing in the morphology of the SPR curve. The behaviors of morphologic parameters of the curve present important knowledge that can be processed by a non-linear estimation method as a key to solve the non-uniqueness problem. A conventional neural network adapted to include these knowledge was the non-linear method chosen.

2.1 Morphology of SPR curve

The incident light excites the phenomenon and is reflected. The reflected light intensity, reflectivity, varying with the monitored parameter is presented by a SPR curve. Among others, the most used interrogation modes (Sousa, 2013) are angular interrogation mode (AIM), in which the incident angle (θ) varies with a constant wavelength (λ), and the wavelength interrogation mode (WIM), in which the incident angle is kept constant and the wavelength varies.

The characteristic SPR curve is shown in Figure 1. There is a maximum reflection of light (tending to total reflection) when the monitored parameter moves away from the resonance condition θ_R or λ_R , depending on the interrogation mode. Next to resonance there is a significant drop in reflected light, but not to zero, despite of what happens in theory. The decrease in reflected

intensity is asymmetric relative to the resonance value: $R(\theta_R + \Delta\theta) \neq R(\theta_R - \Delta\theta)$. The incident light ranges the angles $[\theta_I, \theta_F]$ depending on the configuration used: bio-chip, incident light, photodetectors, or other.

The AIM and WIM curves have the same form and morphological parameters. Besides the resonance angle replaced by the resonance wavelength λ_R . The abscissa axis varies in the range $[\lambda_I, \lambda_F]$.

Different parameters can be extracted from the SPR curve and can be used to characterize its morphology. All these parameters (for AIM) are shown in Figure 1. They are:

Curve energy (E) : The curve energy is calculated by the integral:

$$E = \int_{\theta_I}^{\theta_F} R(\theta) d\theta \quad (\text{AIM}) \quad (1)$$

Curve depth (dip) : The reflected light reduction at resonance condition from total reflection condition. Ideally the reflection in resonance is zero, maximum dip. In real conditions this value ranges from 0.4 to 0.6.

Resonance angle (θ_R) - AIM: The angle at which happens the curve minimum. The resonance angle can be used to calculate the refractive index of the medium if its sensitivity to the layer thickness is ignored. The reflected light is sampled according to the size of the photodetectors and its sensitive region, so that a data processing is used to identify the resonance. Polynomial fit or the calculation of curve centroid through the First Momentum technique are greatly used.

Baseline (BL) : Threshold to discard part of the curve. It is assumed that the points of the curve with values below this threshold are more significant. The most used techniques for this calculation are the full width half maximum value (FWHM) and dynamic baseline (Thirstrup and Zong, 2005).

Curve width (Γ) : The distance between the two points that intersect the baseline is defined as curve width. Also are calculated the horizontal distance between the minimum value θ_R and both the intersection points, by left θ_{BL}^L and right θ_{BL}^R the minimum.

$$\begin{aligned} C_L &= \theta_R - \theta_{BL}^L \\ C_R &= \theta_{BL}^R - \theta_R \\ \Gamma &= C_L + C_R \end{aligned} \quad (2)$$

Asymmetry (G) : The shape of the curve is also studied by its asymmetry about the resonance value:

$$G = C_R/C_L \quad (3)$$

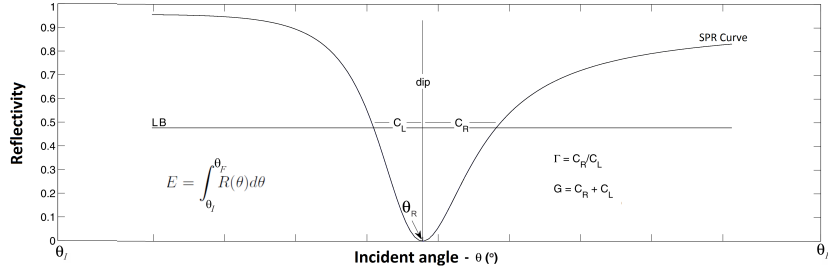


Figure 1: Characteristic curve of the SPR phenomenon (AIM) and relevant morphological parameters: Energy (E), Baseline (BL), Resonance angle (θ_R), depth (dip), width (G) and asymmetry (Γ).

2.2 Simulation

Simulations based on the Fresnel equations model for the SPR phenomenon have been extensively performed adjusting the parameters according to the bio-sensing module of Texas Instrument based on the Spreeta bio-chip (SPREETA, 2000; Meléndez et al., 1997), see Table 1.

Ranging the refractive index from 1.33 to 1.34 at step of $10^{-4}RIU$ and the layer thickness from 0 nm to 100 nm at a step of 1 nm were simulated 10,201 SPR curves. These curves were used in a theoretical study about influence of the biological layer properties (refractive index and thickness) to the SPR curve and its morphological parameters. The monotonicity, concavity and growth of each influence curve were analyzed, according to (Filho, 2006; Filho et al., 2010). The results are summarized in Table 2 for refractive index and Table 3 for thickness variation.

2.3 Multiple prior knowledge neural network (MPKNN).

The tool used to estimate the biological layer properties was a neural network. To solve the non-uniqueness problem, besides increase learning speed and accuracy of the estimation, a neural network in which prior knowledge about the curve morphology could be inserted was selected. The Multiple Prior Knowledge Neural Network (MPKNN) described by (Haichuan et al., 2010) was implemented. The main difference between a MPK neural network and a conventional one is the training method. The chosen network includes

Table 1: SPREETA simulation parameters.

Parameter	Value
Refractive index of the optical substrate	1.48
Refractive index of gold layer (Johnson and Christy, 1972)	$12.19 + 48.5i$
Gold layer thickness	$50nm$
Light wavelength (peak)	$830nm$
External medium refractive index: Water	1.33
Incident angle range (degrees)	64 a 80 step: 0.25

Table 2: SPR curve morphological parameters varying with the biological layer refractive index (n).

Parameter	Growth	Concavity
Energy (E)	Decrease $\partial E/\partial n < 0$	—
Resonance angle (θ_R)	Increase $\partial \theta_R/\partial n > 0$	—
Baseline (BL)	Increase $\partial BL/\partial n > 0$	—
Depth (dip)	Decrease $\partial dip/\partial n < 0$	—
Width (Γ)	Increase $\partial \Gamma/\partial n > 0$	—
Asymmetry (G)	Not Monotonic	—

Table 3: SPR curve morphological parameters varying with the biological layer thickness (d).

Parameter	Growth	Concavity
Energy (E)	Decrease $\partial E/\partial d < 0$	Concave $\partial^2 E/\partial d^2 > 0$
Resonance angle (θ_R)	Increase $\partial \theta_R/\partial d < 0$	Convex $\partial^2 \theta_R/\partial d^2 < 0$
Baseline (BL)	Increase $\partial BL/\partial d > 0$	Convex $\partial^2 BL/\partial d^2 < 0$
Depth (dip)	Decrease $\partial dip/\partial d < 0$	Concave $\partial^2 dip/\partial d^2 > 0$
Width (Γ)	Increase $\partial \Gamma/\partial d > 0$	Convex $\partial^2 \Gamma/\partial d^2 < 0$
Asymmetry (G)	Decrease $\partial G/\partial d < 0$	Convex $\partial^2 G/\partial d^2 < 0$

constrictions while training that are consequence of the prior knowledge to be inserted.

The MPKNN is a three layers neural network with different quantities of neurons per layer. The input (and output) layer have as many neurons as input (or output) variables the network has. The third layer of the MPKNN is a hidden layer with as many neurons as necessary. The hidden layers is composed by linear (4) and nonlinear (5) activation function neurons. So that, each input variable is computed linearly and nonlinearly, if any of these behavior does not fit the variable it is forgotten by the pruning process also implemented. The network is described by (6).

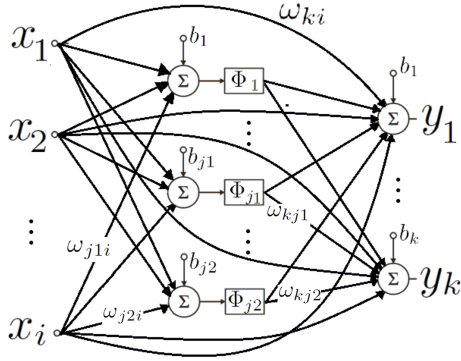


Figure 2: Multiple prior knowledge neural network structure. The neurons up to $j1$ at the hidden layer are non-linear and the others are linear.

$$\Phi_{j2}(x) = x. \quad j2 = m + 1, \dots, j \quad (4)$$

$$\Phi_{j1}(x) = \frac{1}{1 + e^{-x}}. \quad j1 = 1, 2, \dots, m \quad (5)$$

$$y_k = \sum_{j1} \left[\Phi_{j1} \left(\sum_i x_i \omega_{j1i} + b_{j1} \right) \omega_{kj1} \right] + \sum_{j2} \left[\left(\sum_i x_i \omega_{j2i} + b_{j2} \right) \omega_{kj2} \right] + \sum_i \omega_{ki} x_i + b_k, \quad (6)$$

The MPK network structure can be seen in Figure 2. The entries x_i ($i = 1, \dots, 6$) are the normalized morphological parameters of the curve (see Tables (2) and (3)), the outputs y_k ($k = 1, 2$) are the normalized biological properties to be estimated (refractive index and thickness). The data is normalized, or retrieved, in order to have zero mean and unit deviation according to (7).

$$x_i = (X_i - \bar{X}) \delta X \quad (7)$$

The network has a batch training with error calculated by (8), A is the number of samples for training and S the number of outputs of the network, y_T the output of the network being trained and y_R the output data of the training set. The error includes a criterion for pruning the network through bayesian and gaussian functions to evaluate the weights of the internal connections (input-hidden and hidden-output) with (9) and on direct connections (input to output) with (10). Minimizing these errors during training ensures the pruning of the neural network, the redundant or minimally influential weights are reset (deleted), implying in the simpler network as possible.

$$SSE = \sum_a^A \sum_s^S (y_T - y_R)^2, \quad (8)$$

$$E_\omega^c = n1 \log \left(\sum |\omega_{ji}| \right) + n2 \log \left(\sum |\omega_{kj}| \right) \quad (9)$$

$$E_\omega^d = \frac{1}{2} d \log \left(\sum \omega_{ki}^2 \right) \quad (10)$$

being $n1$ the number of connections from the input layer to the hidden layer, ω_{ji} the weight of these connections; $n2$ the number of connections from the hidden layer to the output layer and ω_{kj} the weight of these connections; d the number of hidden layer connections to the output layer and ω_{ki} the weight of these connections.

2.4 Training data and algorithm

The MPKNN training is performed with an algorithm for nonlinear optimization with boundary conditions. The weights must be determined to minimize $SSE + \gamma(E_\omega^c + E_\omega^d)$. Being γ a regularization factor to define the priority level of the pruning criteria.

Prior knowledge is inserted during the training phase. The information presented in Tables 2 and 3 are inserted in training as boundary conditions in the optimization algorithm. Defined y_k at (6), we can define its derivatives of first (11) and second (12) orders. A thickness restriction must be included in training too: $y_2 > 0$.

$$\frac{\partial y_k}{\partial x_i} = \sum_{j1} \omega_{j1i} h_{j1} (1 - h_{j1}) \omega_{kj1} + \sum_{j2} \omega_{j2i} \omega_{kj2} + \omega_{ki} \quad (11)$$

$$\frac{\partial^2 y_k}{\partial x_i^2} = \sum_{j1} \omega_{j1i}^2 h_{j1} (1 - h_{j1}) (1 - 2h_{j1}) \omega_{kj1} \quad (12)$$

$$h_{j1} = \Phi_{j1} \left(\sum_i x_i \omega_{j1i} + b_{j1} \right)$$

A sequential quadratic programming algorithm (SQP) (Nocedal and Wright, 1999) meets training needs of the network.

The lack of experimental data already characterized difficulties the network training and validation of the results. The network training was conducted with 2,500 simulated curves with refractive index ranging from 1.3301 to 1.3350 at a step of $10^{-4} RIU$ and layer thickness ranging from 1 to 50 nm. Also, 500 experimental curves for water were used in training. It was possible only because when the biological layer and the external layer are the same, the three layers is enough to characterize the entire the system, and this model is entirely known.

The training data was divided in *training set*, used calculate the weights, *evaluate set*, used to evaluate the if the training is finished or another interaction is needed and *performance set*, used to evaluate the performance of the already trained network, analyzing if the training was not super specialized, fitting only to the training set.

3 Results

The Many factors influence the neural network performance. The most important ones are pa-

Table 4: Mean error of neural network training for different values of γ .

Regularization factor γ	Average percentage error	
	n_3	d_3
10	0.0054	1.1098
5	0.0014	0.9297
2	0.0015	0.8631
1	0.0013	0.9135
0.5	0.0013	0.9169
0.25	0.0059	1.0371

parameters chosen by the user: (i) the regularization factor (γ), (ii) the number of neurons in the hidden layer, (iii) data organization. The influence of each one of these factors was studied separately in order to find the optimal network.

The influence analysis of performed keeping constant two parameters and varying the third. For each parameter combination the training epoch was performed and evaluated calculating the average error of the *performance data set*. The training epoches were repeated as many times as needed to the performance analyzes result in an average error variation less than

3.1 Regularization factor

The neural network was trained to $\gamma = 10, 5, 2, 1, 0, 5, 0.25$, with a constant number of ten neurons at the hidden layer, half linear and half non-linear. The average error obtained in each network can be seen at Table 4. Although a small difference, the smallest deviation results were for $\gamma = 1$ and $\gamma = 2$. The criteria adopted to choose the γ value was the one that minimizes the error layer thickness estimation, since the magnitude of its deflection is much larger than the deviation of the refractive index.

3.2 Hidden layer neurons

Experiments were performed with the chosen regularization factor $\gamma = 2$ and varying the number of neurons at the hidden layer hidden: six, eight and ten, always half linear and half nonlinear. No significant difference in results was observed, however. Profit attributed to the pruning performed by (9) and (10). So that, the network with six neurons was chosen only to reduce the complexity the network by approximately a third.

3.3 Data organization

The network convergence and response were also evaluated for different input data. Morphological data from the SPR curve were evaluated when calculated by different methods. Two baseline algorithms: FWMH and dynamic baseline. And two minimum search algorithms: polynomial fit and the first momentum. The results are shown in Table 5.

Defined the optimal neural network, it was trained with mainly simulated data and experimental data from water. The resulting MPKNN was applied to 5000 data samples generated by a one-hour experiment alternating the analyzed solution: water and a 50% PBS (*Phosphate Buffered Saline*) solution with refractive index of $1.5 \times 10^{-3} RIU$. The PBS layer thickness could not be measured, so that, this data could neither be used in training neither there were a expected estimated value. The PBS solution only generates reversible bind with gold, which can be removed with just water. The MPKNN estimated values are presented through a sensorgram in Figure 3.

4 Discussion

The experiment produced results very close to the expected ones. When applied to simulated data the error was less than 1%. Experimental data produced results of refractive index averaging near of $1.5 \times 10^{-3} RIU$ when the analyte was exchanged. The layer thickness estimative approaches to a null thickness layer when water is in the bio-sensor, that is, a three layer model, as used in training. The actual layer thickness is unknown, so, to validation of results, the reverse process was performed. A simulated curve was generated with the estimated data, its result was consistent with the experimental curve.

5 Conclusions

A correctly trained neural network allows to monitor the biological layer, knowing in real-time its parameters, refractive index and thickness. This information permits to identify when the layer is fully formed or its wear. A quantitative evaluation of the estimated solution requires more study and experimentation. However, the results allowed a qualitative response, allowing the user to identify when layer formation is already complete and monitor its wear. It permits to faster prepare the biosensor for measures, with no solutions wastes or wrong data due to an not complete layer.

Acknowledgments

The authors would like to thank PPgEE/UFCG, CAPES and CNPq for the financial support and research grants.

Referências

de Bruijn, H. E., Altenburg, B. S., Kooyman, R. P. and Greve, J. (1991). Determination of thickness and dielectric constant of thin transparent dielectric layers using surface plasmon resonance, *Optics Communications* **82**(5-6): 425–432.

Table 5: Evaluation of neural network for different techniques combinations to calculate the morphological parameters.

Techniques		Mean error (%)		Maximum error (%)	
Baseline	Minimum search	n_3	d_3	n_3	d_3
Dynamic	First Momentum	0.0015%	0.8631%	0.0160%	1.1423%
Dynamic	Polynomial Fit	0.0058%	1.0901%	0.0181%	1.7817%
FWHM	First Momentum	0.0068%	1.3163%	0.0228%	2.6901%
FWHM	Polynomial Fit	0.0082%	3.6581%	0.0252%	5.4979%

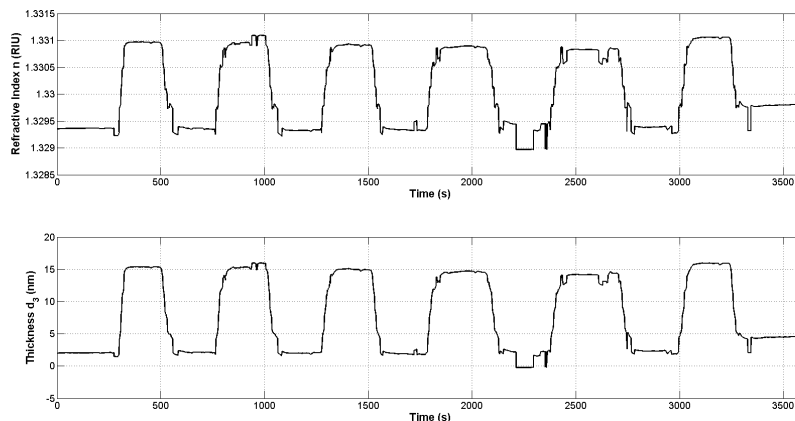


Figure 3: Results obtained for the neural network applied to experimental data.

- Filho, C. A. S. (2006). *Desenvolvimento de um sistema eletrônico de aquisição e processamento para biosensores.*, Master's thesis, UFCG - Universidade Federal de Campina Grande.
- Filho, C. A. S., Lima, A. M. N., Moreira, C. S., Thirstrup, C. and Neff, H. (2010). Line shape analysis and extended instrumental operation of surface plasmon resonance sensors, *Plasmonics* (5): 259–266.
- Haichuan, L., Hongye, S., Lei, X., Yong, G. and Gang, R. (2010). Multiple-prior-knowledge neural network for industrial processes, *Automation and Logistics (ICAL), 2010 IEEE International Conference on*, pp. 385–390.
- Homola, J. (2003). Present and future of surface plasmon resonance biosensors, *Anal Bioanal Chem*.
- Johnson, P. B. and Christy, R. W. (1972). Optical constants of the noble metals, *Physical Review B* **6**(12).
- Johnston, K. S., Karlsen, S. R., Jung, C. C. and Yee, S. S. (1995). New analytical technique for characterization of thin films using surface plasmon resonance, *Materials Chemistry and Physics* **42**(4): 242–246.
- Meléndez, J., Carr, R., Bartholomew, D., Taneja, H., Yee, S., Jung, C. and Furlong, C. (1997). Development of a surface plasmon resonance sensor for commercial applications, *Sensors and Actuators B: Chemical* (38-39): 375–379.
- Nocedal, J. N. and Wright, S. J. (1999). Numerical optimization, *Prentice Hall* p. Caps. 12 e 18.
- Peterlinza, K. and Georgiadis, R. (1996). Two-color approach for determination of thickness and dielectric constant of thin films using surface plasmon resonance spectroscopy, *Optics Communications* (130): 260–266.
- Phelps, J. M. and Taylor, D. M. (1996). Determining the relative permittivity and thickness of a lossless dielectric overlayer on a metal film using optically excited surface plasmon polaritons, *Journal of Physics D: Applied Physics* (Vol. 29, No. 4): 1080–1087.
- Sousa, T. A. T. (2013). *Contribuição ao estudo de técnicas de extração de parâmetros para bio-sensores ópticos.*, Master's thesis, UFCG - Universidade Federal de Campina Grande.
- SPREETA (2000). *TSPR1A170100: SpreetaTM Liquid Sensor*, Texas Instruments, Dallas, Texas.
- Thirstrup, C. and Zong, W. (2005). Data analysis for surface plasmon resonance sensors using dynamic baseline algorithm, *Sensors and Actuators B: Chemical* (106): 796–802.
- Zhang, J. and Wang, G. P. (2009). Determination of thickness and dielectric constant of thin films by dual-wavelength light beaming effect of a metal nanoslit, *Journal of Applied Physics* **106**(3): 034305.